Separation and Purification Technology 342 (2024) 126885

Contents lists available at ScienceDirect

Separation and Purification Technology

journal homepage: www.elsevier.com/locate/seppur

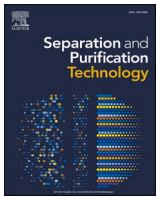

Selective electrodialysis: Targeting nitrate over chloride using PVDF-based AEMs

Daniele Chinello [a,b], Louis C.P.M. de Smet [a,b,*], Jan Post [a]

[a] Wetsus, European Centre of Excellence for Sustainable Water Technology, Oostergoweg 9, Leeuwarden 8911 MA, the Netherlands
[b] Advanced Interfaces & Materials, Laboratory of Organic Chemistry, Wageningen University, Stippeneng 4, Wageningen 6708 WE, the Netherlands

ARTICLE INFO

Keywords:
Ion separation
Nitrate over chloride selectivity
Monovalent selective electrodialysis
PVDF-based anion-exchange membranes

ABSTRACT

The depletion of natural resources and the escalating environmental concerns associated with pollution necessitate innovative approaches for sustainable resource management. In this study, we investigated the selective separation of nitrate from chloride in electrodialysis (ED) using a recently introduced PVDF-based anion-exchange membrane (PVDF-50) and two commercially available membranes (ACS and AMX from Neosepta). Experimental ED data show that the membrane PVDF-50 presents a higher value of nitrate over chloride selectivity compared with the two commercial membranes, the highest reported in literature.

However, recognizing that completely preventing the permeation of chloride ions into the concentrate stream was not feasible, we explored the potential of a system in which anion-exchange membranes presenting different monovalent selectivity were alternated. In this approach, referred to as nitrate-selectrodialysis (NO_3-SED), the different selectivity of PVDF-50 and AMX membranes was leveraged to demonstrate the possibility of increasing nitrate concentration, while simultaneously reducing chloride levels in a stream. This approach proves highly advantageous in applications where mitigating chloride contamination is a significant concern while recovering nitrate.

1. Introduction

Nitrate, a key source of nitrogen for plants, plays a crucial role in promoting agricultural productivity and ensuring adequate food production to sustain a growing global population [1]. It is a fundamental component of fertilizers, facilitating the enhanced growth of crops and bolstering agricultural yield [2,3]. However, excessive use of nitrogen-based fertilizers has led to a range of environmental issues, notably eutrophication. Eutrophication occurs when excess nitrogen enters water bodies, stimulating excessive growth of algae and other aquatic plants, ultimately degrading water quality and disrupting ecosystems [4]. To mitigate this, denitrification systems are employed to reduce nitrogen levels in wastewater and prevent its adverse impact on the environment. Denitrification involves converting nitrate into nitrogen gas [5,6], which can be released harmlessly into the atmosphere. While effective, this approach may not be the most efficient, as it leads to the loss of valuable nitrogen and necessitates the subsequent replenishment of nitrogen-based fertilizers. On the other hand, selective separation of nitrate offers a more convenient solution by allowing for the recycling of nitrate and can have potential application such as in industry [7] or greenhouses [8].

Electrodialysis can effectively remove nitrate ions by utilizing ion-exchange membranes. However, a challenge remains when also other monovalent ions are present in the water, such as chloride, because of their similar physicochemical properties (Table 1). Therefore, the need for advancements in membrane technology to develop selective nitrate membranes is pivotal to achieve responsible nitrate management while enabling the recycling of this important nutrient.

A strategy to increase the membranes selectivity towards ions possessing the same valence is based on exploiting the difference in dehydration energy of the ions [9–12]. Several studies [13–15] have demonstrated that increasing the membranes' hydrophobicity can promote the selective transport of ions with lower hydration energy, such as nitrate (Table 1). This approach has also been explored for the selective separation of monovalent cations like sodium and potassium [16–18]. Ions with a reduced hydration energy undergo easier dehydration, thereby reducing the energy barrier for their transport from the solution into the membrane [19,20]. Moreover, less hydrated ions can interact

* Corresponding author at: Advanced Interfaces & Materials, Laboratory of Organic Chemistry, Wageningen University, Stippeneng 4, Wageningen 6708 WE, The Netherlands.
E-mail address: louis.desmet@wur.nl (L.C.P.M. de Smet).

https://doi.org/10.1016/j.seppur.2024.126885
Received 14 December 2023; Received in revised form 19 February 2024; Accepted 21 February 2024
Available online 23 February 2024

Table 1
Ionic radii, hydrated radii and hydration energies of nitrate and chloride [39].

Anion	Ionic radius [nm]	Hydrated radius [nm]	Hydration energy [kcal·mol^{-1}]
Nitrate (NO_3^-)	0.264	0.335	71
Chloride (Cl^-)	0.181	0.332	81

easily with the fixed charged group in the membrane [19,21], further lowering the energy barrier. At the same time, the hydrophobicity of the fixed charged groups can be increased, further enhancing selectivity [22–26].

However, the precise ion-transport mechanism within a membrane is intricate, and most likely, the membrane's selective behavior results from multiple mechanisms operating simultaneously. Indeed, other studies suggest that increasing the membrane's hydrophobicity also influence the ion sieving properties of the membrane, thereby leading to a selective behaviour [18,27–30]. Specifically, more hydrophobic membranes exhibit lower water uptake and degree of swelling, which in turn influence the size of the nanochannels in the membranes. Consequently, when the hydrated radii of the ions are comparable to the pores size of the nanochannels, dehydration is required for the transport of ions through the membrane and hence ions presenting lower hydration energy permeate easily [28,31,32].

Also, the hydrophobic/hydrophilic nature of the membranes may influence the characteristics of the ionic pathway, affecting the ions mobility within the membrane and thus the selectivity [13,20].

In our previous research [33], we studied the transport of nitrate and chloride using newly developed PVDF-based anion-exchange membranes. Specifically, we explored the impact of varying the PVDF content within the membranes (ranging from 0 to 50 wt%), using a ionomer solution (Fumion FAS-24, FUMATECH BWT GmbH) in combination with PVDF. Our results indicated an enhanced nitrate transport upon increasing PVDF concentration, with the membrane containing 50 wt% PVDF exhibiting the highest nitrate transport. Building on these findings, we decided to investigate the performance of this membrane in comparison to two commercially available membranes (ACS, a monovalent selective membrane, and AMX, a standard grade membrane, from Neosepta) in an electrodialysis (ED) system, presenting the results in this current study. Additionally, we also investigated the potential of a proposed approach called nitrate-selectrodialysis (NO_3-SED), leveraging the differences in nitrate over chloride selectivity of various membranes to achieve concurrent nitrate concentration and chloride depletion in a stream. The approach of alternating a series of cation or anion-exchange membrane in a stack has been explore in literature for various applications such as the separation of divalent from monovalent ions[34–36], selective production of carboxylic acids [37], and recovery of L-lysine from L-lysine monohydrochloride [38]. Nevertheless, to the best of our knowledge, this study introduces a novel application of this system, specifically targeting the challenging separation of two monovalent ions

2. Materials and methods

2.1. Chemicals

Polyvinylidene fluoride (PVDF) (average M_w ~ 534,000 by GPC, powder form), sodium chloride (ACS reagent, ≥99.0 %), sodium nitrate (ACS reagent, ≥99.0 %), sodium sulphate (ACS reagent, ≥99.0 %, anhydrous), were purchased from Sigma Aldrich and used without any further treatment. N-methyl-2-pyrrolidone (NMP, HPLC grade 99.5 %) was purchased from Alfa Aesar. Fumion FAS (24 wt% solution in NMP), which physicochemical properties are reported in **Table S1** of the Supporting Information, was purchased from FUMATECH BWT GmbH, Bietigheim-Bissingen, Germany. The Neosepta AMX, ACS, and CMX membranes were purchased from ASTOM Corporation, Tokyo, Japan. The chemical composition and physical properties of Neosepta AMX and ACS are reported in Table 2.

2.2. PVDF-based AEM fabrication

The PVDF-based AEM was manufactured by mixing in NMP, PVDF and Fumion FAS-24 in a weight ratio of 50:50. The resulting mixture, with a concentration of polymers of 16 wt%, was stirred overnight to achieve complete dissolution prior casting it onto a glass plate kept at 60 °C for 24 h, in order to remove the solvent by evaporation. To additionally guarantee thorough solvent elimination, the membranes were immersed in a 0.5 M NaCl solution for a duration of 2 h. This process was reiterated five times, with each repetition involving the replacement of the solution. The wet membrane thickness was then measured using a digital thickness gauge (Mitutoyo Corporation, model no. ID-C112BS) and stored in a 0.5 M NaCl solution. The membrane was labelled PVDF-50, in order to indicate the percentage of PVDF, and selected characteristics, together with those of the commercial anion-exchange membranes used in this study, are reported in Table 2.

2.3. Membrane characterization

2.3.1. Ion-exchange capacity (IEC)

The ion-exchange capacity (IEC) of an ion-exchange membrane refers to the amount of ions, expressed in milliequivalents per gram (meq·g^{-1}) that the membrane can exchange, and it is an indirect measure of the membrane's fixed charge density. The procedure to measure the IEC involves conditioning the membrane in 0.5 M NaCl for 48 h and then transferring it in 0.5 M $NaNO_3$, the exchange solution. After 24 h, the chloride concentration was evaluated using ion chromatography and then the IEC was calculated using the following equation [40]:

$$IEC = \frac{n_{eq}}{W_{dry}} \quad (1)$$

where n_{eq} refers to the equivalent of exchanged ions (eq) and W_{dry} (g) to the membrane's dry mass.

2.3.2. Water uptake

The water uptake of the membranes was measured as follows. The membranes were immersed in demineralized water for 24 h, and then weighted after removing the water from the surface with a tissue. After recording the wet membrane mass (W_{wet}, in grams), the membranes were placed in an oven at 55 °C for 24 h in order to achieve complete water evaporation. The water uptake was then calculated after measuring the dry membrane mass (W_{dry}, in grams), using the following

Table 2
Chemical and physical properties of the membranes used in this study: PVDF-50, AMX, ACS, and CMX.

Membrane	Composition	Thickness (μm)	IEC (meq·g^{-1})	Water Uptake (%)
PVDF-50	PVDF:Fumion FAS-24 = 50:50	80–85	0.7	7
AMX	Styrene-divinyl benzene reinforced with PVC [47]	140	2.1	22
ACS	Styrene-divinyl benzene reinforced with PVC, with highly cross-linked layer on both of the membrane surfaces [47]	120	1.9	26
CMX	Cross-linked sulfonated styrene–divinylbenzene copolymer (45–65 %) and polyvinylchloride (45–55 %) [48]	150	2.5	30

equation:

$$Wateruptake = 100 \times \frac{W_{wet} - W_{dry}}{W_{dry}}\% \quad (2)$$

2.3.3. Contact angle

The hydrophobicity of the membranes under investigation was evaluated by measuring the contact angle through the captive bubble method. This technique involves measuring the contact angle formed between an air bubble (1 μL) and the surface of the membrane immerse in water. This angle is indicative for the hydrophobicity of the surface. A higher contact angle indicates a higher hydrophobicity, meaning the material is less likely to interact with or be wetted by water. Conversely, a lower contact angle indicates a more hydrophilic surface, indicating a higher affinity for water. Contact angles were determined using a contour analysis system (OCA35, DataPhysics Instruments, Germany), and six measurements were taken for each membrane, varying the position of each measurement.

2.3.4. Permselectivity

The permselectivity of an ion-exchange membrane refers to its ability to selectively allow the passage of counter-ions, ions with the opposite charge of the fixed group within the membranes, while blocking the co-ions, ions with the same charge. The permselectivity was determined following previous contribution in literature [40,16,33] by recording the potential across the membrane separating two electrolyte solution such as NaCl 0.1 M and NaCl 0.5 M, which are recirculated in the system at a flow of 750 mL·min^{-1}. Two Ag/AgCl electrodes immersed in the solutions where used to record the potential after reaching the steady state. The membrane permselectivity expressed as a percentage is then calculated by the following equation:

$$a = 100 \times \frac{\Delta V_{measured}}{\Delta V_{theoretical}}\% \quad (3)$$

where $\Delta V_{theoretical}$ represents the theoretical membrane potential calculated according to the Nernst equation for a membrane 100 % selective towards counter-ions.

2.3.5. Permeability coefficients ratio

The permeability coefficients ratio of ion-exchange membranes is a parameter that characterizes the affinity between the membranes and the counter-ions present in a solution. It can be determined by measuring the zero-current potential existing across a membrane separating two electrolyte solutions containing the same co-ion but different counter-ion (in our case Na^+, and NO_3^- and Cl^-, respectively). It can be used to get a quick indication of the selective behavior of the membranes toward target ions, *e.g.* nitrate *vs.* chloride. The permeability coefficients ratio was determined according to a procedure we published earlier [33]. The potential across the membrane ($\Delta\Psi$) separating two electrolyte solutions such as 0.1 M NaCl and 0.1 M $NaNO_3$ recirculating at a flow rate of 750 mL·min^{-1} was recorded using two Ag/AgCl electrodes immersed in the solutions for a period of 40 min. The potential used for the calculations is the average of the values recorded once the steady state was reached, after *ca.* 10 min, and it is related to the permeability coefficients of the counter-ions by the Nernst equation:

$$\Delta\Psi = \frac{RT}{F} ln \frac{P_{NO_3^-}[NO_3^-]}{P_{Cl^-}[Cl^-]} \quad (4)$$

where F is the Faraday constant (96,458 A·s·mol^{-1}), R is the universal gas constant (8.314 J·mol^{-1}·K^{-1}), T is the absolute temperature (K), $P_{NO_3^-}$ and P_{Cl^-} are the permeability coefficients of the counter-ions, and $[NO_3^-]$ and $[Cl^-]$ are the concentrations of the ions in each compartment.

Considering that the concentration of nitrate and chloride is the same, rearranging **Equation (4)** enables the determination of the permeability ratio using the following equation:

$$\frac{P_{NO_3^-}}{P_{Cl^-}} = e^{\frac{F\Delta\Psi}{RT}} \quad (5)$$

2.4. Membrane performance

2.4.1. Electrodialysis experiments

The electrodialysis (ED) setup used in this study to determine the nitrate over chloride selectivity of the anion-exchange membranes under investigation (PVDF-50, ACS, and AMX), is schematically represented in Fig. 1. The configuration consists in a sequence of five ion-exchange membranes arranged as follows: three cation-exchange membranes (CMX from Neosepta) alternated with two anion-exchange membranes. This configuration results in a total of two cell pairs, each consisting of a cation and an anion-exchange membrane, separating a diluate and concentrate stream. The IEM area available for the ion transport is 20 cm^2, and each membrane is separated from the other by a spacer-integrated gasket with a thickness of 0.5 mm. The setup is equipped with platinum-coated titanium mesh electrodes, and the compartments are separated from each other by a cation-exchange membrane (CMX), in order to prevent the migration of chloride ions towards the anode, thereby avoiding chlorine formation. The electrode compartments maintain a recirculating solution of 0.05 M Na_2SO_4; in the outlets of these compartments two Ag/AgCl electrodes connected to the potentiostat are placed to measure the potential across the five membranes.

The experiments are conducted in batch-mode at a current density of 20 A·m^{-2}, with a potentiostat (Autolab AUT72157, Metrohm) used as current supplier. The solutions recirculating in the concentrate and dilute compartments are equimolar solutions of NaCl and $NaNO_3$ with a total concentration of anion of 0.1 M and a volume of 0.1 L each. The duration of each experiment is 3 h, which results in a theoretical total anion removal from the diluate stream of 90 %. For each membrane, experiments were repeated three times to assess reproducibility.

In order to evaluate the nitrate over chloride selectivity over time, samples were taken every 30 min and analysed by ion chromatography (IC) to determine the ion concentrations. The concentrations obtained were first used to calculate the transport number (t), which refers to the fraction of current transported by a specific ion, and for a monovalent ion (i) is calculated using the following equation:

$$t_i = \frac{FV}{iAN} \times \frac{\Delta C_i}{\Delta t} \quad (6)$$

where F is the Faraday constant (96,458 A·s·mol^{-1}), V (m^3) and ΔC_i (mol·L^{-1}) are respectively the volume and the variation of the ion concentration in the concentrate stream, A (m^2) the surface membrane area, N the number of cell pairs, Δt (s) is the time of the experiments, and i is the current density applied (A·m^{-2}). The current efficiency of the experiments is defined by the equation:

$$\eta = (J_i + J_j)\frac{F}{i} \quad (7)$$

where J_i and J_j are the ionic fluxes across the membrane expressed in mol·m^{-2}·s^{-1} of the ions under consideration, which are calculated using the equation:

$$J_i = \frac{V}{AN} \times \frac{\Delta C_i}{\Delta t} \quad (8)$$

In order to compare our results with other studies, the nitrate over chloride selectivity over time of the membranes under investigation was calculated according to the following equation reported by Mubita *et al.* [41]:

$$S_{Cl^-}^{NO_3^-} = \left(\frac{\Delta C_{NO_3^-}}{\Delta C_{Cl^-}}\right)_{Concentrate} \times \left(\frac{C_{Cl^-}}{C_{NO_3^-}}\right)_{Diluate} \quad (9)$$

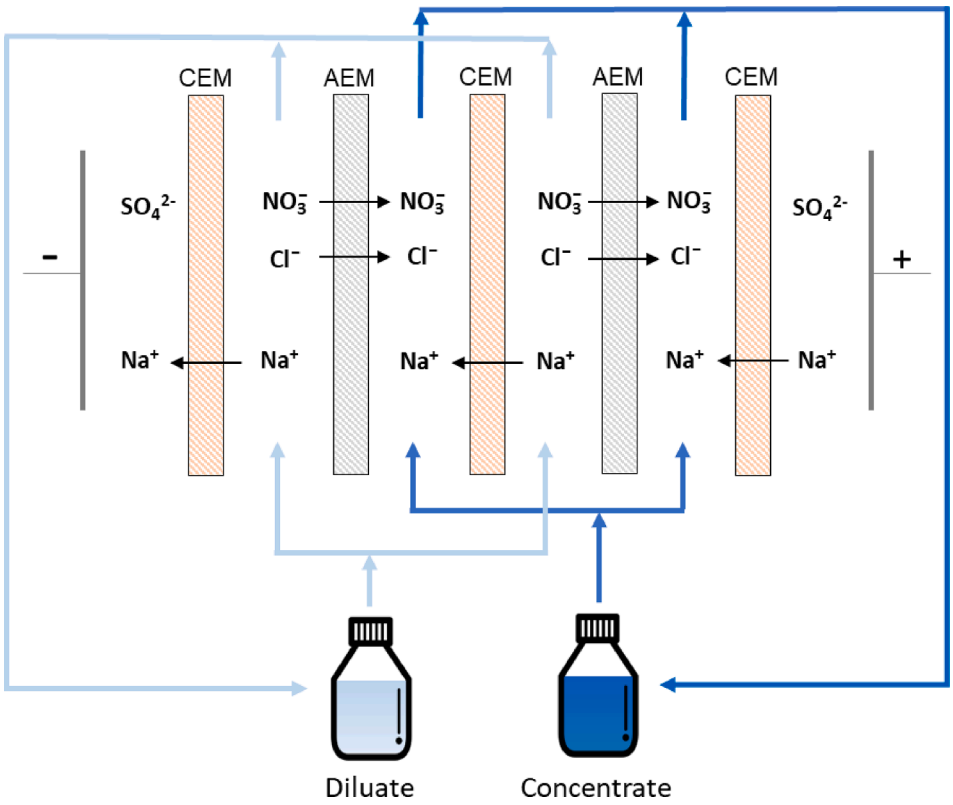

Fig. 1. Schematic representation of the ED setup used to assess the nitrate over chloride selectivity of the anion-exchange membranes PVDF-50, ACS, and AMX. The system is composed of five membranes in total, three Cation-Exchange Membranes (CEMs) and two Anion-Exchange Membranes (AEMs). The experiments are performed in batch-mode, with the concentrate and diluate streams pumped from the reservoirs. The electrodes are from platinum-coated titanium and a Na_2SO_4 solution was recirculated in the electrode compartments.

where $\Delta C_{NO_3^-}$ and ΔC_{Cl^-} refer to the variation of the concentration of nitrate and chloride in the concentrate reservoir between two samples and $C_{NO_3^-}$ and C_{Cl^-} refer to the concentration of the ions in the diluate compartment.

From an application point of view, the recovery ratio is another parameter of interest, which for an ion (i) is defined by Chen *et al.* [42] as:

$$R_i = \frac{V_{ct}(C_{ct} - C_{c0})}{V_{d0}C_{d0}} \times 100 \quad (10)$$

where C_{ct}, C_{c0} and C_{d0} are the concentrations of the ion at time t and 0 respectively in the concentrate and diluate stream, and V_{ct} and V_{d0} are the volume in the concentrate and dilute at time t and zero, respectively.

The energy consumption (E) was evaluated as kilojoules per gram of nitrate recovered following the equation:

$$E = \frac{\Delta V_{stack} \cdot i \cdot A \cdot \Delta t}{\Delta n_{NO_3^-} \cdot MW_{NO_3^-}} \quad (11)$$

where ΔV_{stack} is the average stack potential (V), i is the current density applied ($A \cdot m^{-2}$), A the surface membrane area (m^2), Δt is the time of the experiments (s), $\Delta n_{NO_3^-}$ is the variation in moles of the nitrate in the concentrate stream, and $MW_{NO_3^-}$ the nitrate's molecular weight ($g \cdot mol^{-1}$).

Lastly, in order to assess any dependency of the current applied on its performance, membrane PVDF-50 has also been tested at an increased current density of 40 $A \cdot m^{-2}$.

2.5. Nitrate-selectrodialysis (mSED) experiments

Based on the conventional electrodialysis approach, chloride ions also permeate into the concentrate stream, and in applications [7] where the nitrate recycling should be paired with the simultaneous chloride removal, other membranes configurations might be more beneficial. For this reason, we investigated the potential of a system referred to as nitrate-selectrodialysis (NO_3-SED), which schematic configuration is reported in Fig. 2.

This system capitalizes on the different nitrate over chloride selectivity of two distinct anion-exchange membranes (PVDF-50 and AMX). By strategically alternating between these membranes, we exploit the superior permeability of nitrate ions through PVDF-50 compared to AMX and, conversely, the higher permeability of chloride ions through AMX. Consequently, over time, in Feed 2, the nitrate concentration increases and chloride concentration decreases, while in Feed 1, chloride concentration increases and nitrate concentration decreases.

The experimental settings are similar to those of ED experiments: two platinum-coated titanium mesh electrodes, separated from the AEMs by two CMX membranes, are present with a recirculating solution of 0.05 M Na_2SO_4. The composition of Feed 1 and Feed 2 is 0.05 M NaCl + 0.05 M $NaNO_3$ with a volume of 0.1 L per each feed. A spacer-integrated gasket with a thickness of 0.5 mm was used to separate the membranes and each experiment was conducted in batch-mode lasting for 3 h. Regarding the current density applied, we decided to investigate the performance of the system at two different values: 20 $A \cdot m^{-2}$, and 40 $A \cdot m^{-2}$. The variation of the concentration in the reservoirs of Feed 1 and Feed 2 is monitored over time by taking samples every 30 min and analysing them using ion chromatography. The energy consumption of each experiment have been calculated using the equation:

$$E = \Delta V_{stack} \cdot i \cdot A \cdot \Delta t \quad (12)$$

where ΔV_{stack} is the average stack potential (V), i is the current density applied ($A \cdot m^{-2}$), A the surface membrane area (m^2), Δt is the time of the

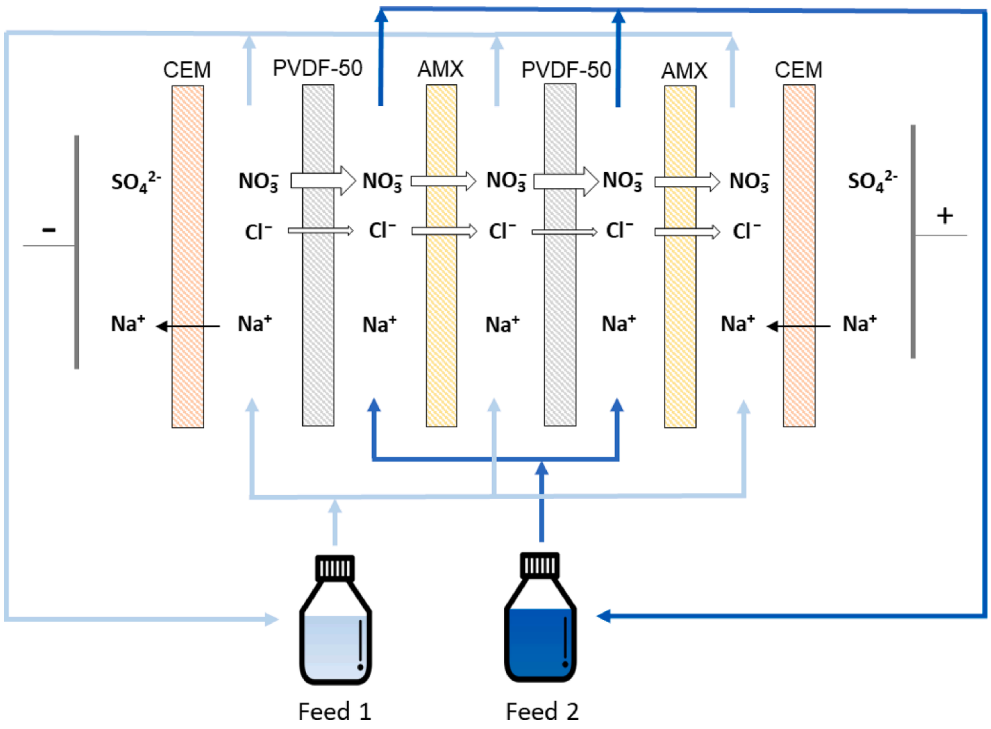

Fig. 2. Schematic representation of the nitrate-selectrodialysis (NO_3-SED) setup used in this study. The system is composed of six membranes in total, two Cation-Exchange Membranes (CEMs) near the electrodes and four Anion-Exchange Membranes (AEMs) in between, featuring an alternating arrangement of two PVDF-50 membranes and two AMX membranes. The experiments are performed in batch-mode, with the Feed 1 and 2 streams pumped from the reservoirs. The electrodes are from platinum-coated titanium and a Na_2SO_4 solution was recirculated in the electrode compartments.

experiments.

3. Results and discussion

3.1. Membrane characterization

3.1.1. IEC and water uptake

Table 2 presents the IEC and water uptake values for the three membranes, which were determined following the procedures described in Sections 2.3.1 and 2.3.2. Notably, the IEC values exhibit the following order: AMX > ACS > PVDF-50. Conversely, the water uptake values follow a different trend: ACS > AMX > PVDF-50. It is worth noting that while we expected a similar trend between IEC and water uptake, the water uptake values of AMX and ACS align with previous findings in the literature [43].

Indeed, the water uptake of a membrane is directly correlated with the proportion of charged groups within the membrane. Elevated quantities of charged groups, resulting in high values of the IEC, result in a higher osmotic pressure and thus a higher water uptake of the membrane [23,44]. However, the water content is also influenced by other parameters, such as the affinity between the polymer matrix of the membrane and water [23], and the presence of reinforcing materials [45]. Typically, the membrane's water absorption capacity depends on the number of hydrophilic groups it contains. When there is low water uptake, it suggests that hydrophobic membrane groups are more prevalent than their hydrophilic counterparts [46].

3.1.2. Contact angle analysis

In an attempt to obtain more insight in the hydrophobic properties of the membranes, drops of water were placed on each membrane. However, quantification of the contact angles turned out to be very difficult as the membranes curled up. Instead, the captive bubble method, a configuration that allows the membranes to be wetted, turned out to be a suitable alternative. Fig. 3 displays the contact angle values measured

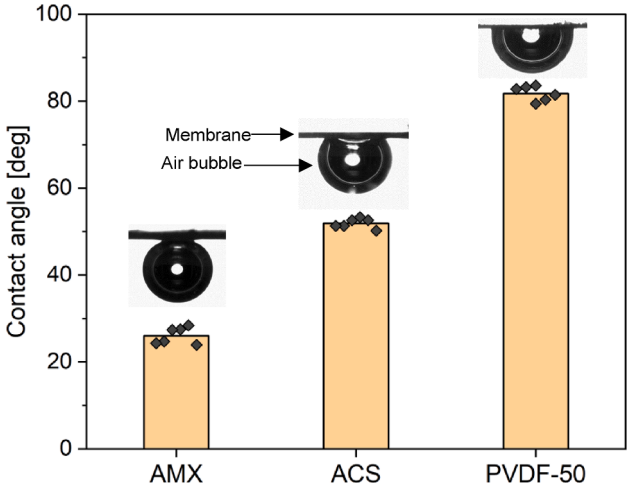

Fig. 3. Contact angle measured by the captive bubble method for the three membranes investigated in this study: AMX, ACS, and PVDF-50. Optical images of the membranes and the air bubble are provided for enhanced clarity.

using this method for the three membranes under investigation in the study: AMX, ACS, and PVDF-50. As becomes clear from these data, the contact angle, and with that the hydrophobicity, increases in the order of PVDF-50 > ACS > AMX.

3.1.3. Permselectivity and permeability coefficients ratio

From the results presented in Fig. 4, it is evident that, across all three membranes, the permselectivity values are consistently around 90 %, aligning with previous findings in the literature [49]. When it comes to the permeability coefficients ratio, a key indicator of a membrane's affinity for nitrate or chloride, we observe that the ratio is consistently larger than 1 for all membranes. This means that all three membranes

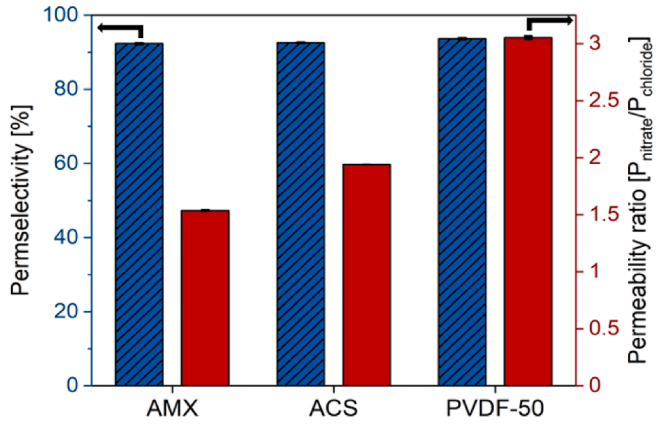

Fig. 4. Permselectivity and permeability coefficient ratio values of the investigated membranes: AMX, ACS, and PVDF-50. Experiments have been repeated three times.

exhibit a preference for nitrate over chloride ions. The values of the permeability coefficients ratio follow the trend of PVDF-50 > ACS > AMX, indicating that PVDF-50 exhibits the highest selectivity for nitrate over chloride, while AMX is the least selective among the three membranes. Comparison of the permselectivity and permeability coefficients ratio results of the AMX and PVDF-50 membranes with those obtained in our precedent study [33], affirms the high reproducibility of the proposed methods for determining these parameters.

3.2. Membrane performance

3.2.1. Selective separation in batch-mode electrodialysis

In accordance with the experiment details outlined in Section 2.4, we present the experimental results of the transport of nitrate and chloride through the three membranes under investigation, PVDF-50, ACS, and AMX, obtained in batch-mode electrodialysis. The concentrations of nitrate and chloride in the two reservoirs were monitored over time (Fig. 5) for the PVDF-50 membrane (for the other membranes, see Supporting Information **Fig. S1**), and, as expected, they increased in the concentrate reservoir while decreasing in the diluate one. Additionally, we observed that in the concentrate reservoir, the concentration of nitrate increased more rapidly over time compared to chloride for all membranes under examination. However, upon analyzing the average ionic flux of nitrate and chloride for the three membranes (Fig. 6), it became evident that PVDF-50 transports more nitrate and less chloride compared to ACS and AMX, indicating a higher selectivity for nitrate. The current efficiency for all experiments was in the range of 91–94 %.

We further assessed the nitrate over chloride selectivity of the three membranes over time using Equation (7) (Fig. 7). The data clearly shows that PVDF-50 presents higher selectivity values compared to ACS, which in turn presents higher values than AMX. Moreover, the selectivity was found to change in time due to changes in the actual concentration ratio in the diluate stream, a trend that has also been reported by Mubita *et al.* [41]. Their work involved both theoretical and experimental investigations into the nitrate over chloride selectivity of three anion-exchange membranes, two commercial, AMX from Neosepta and Ralex AMH-PES from Mega a.s. (Czech Republic), and one heterogeneous AEMs manufactured with a ion-exchange resin featuring quaternary ammonium groups with propyl substituents. The theoretical analysis revealed a significant time dependency of the selectivity, while the reported experimental results showed a less pronounced decrease. Notably, the experimental outcomes for the AMX membrane exhibited a similar trend to our data. Conversely, in the reported case of the Ralex AMH-PES membrane, the selectivity demonstrated an increase over time. Furthermore, the examination of their manufactured anion-exchange membrane with a thickness of 70 μm disclosed a pronounced decrease in selectivity over time, aligning with the theoretical trend. However, the study does not provide an explanation for the observed trends.

Our analysis is based on the equation used to calculate the selectivity (**Equation (9)**), widely employed in literature [9,13,22,27,41,47,50,51], which might present limitations. Specifically, the second term of the equation refers to the concentration of chloride and nitrate at the membrane surface on the diluate stream, typically approximated to the concentration in the bulk solution [9]. We hypothesize that phenomena such as concentration polarization may occur, leading to an inaccurate definition of the concentration at the membrane surface on the desalting side and thus selectivity. This effect becomes more pronounced for higher degrees of desalination [52]. However, given the significance of comparing our results with existing literature, we decided to adopt the selectivity definition provided by Mubita *et al.* in their study.

By analyzing our data is possible to observe that for the membranes ACS and AMX, the selectivity decreases nearly linearly with time, while for PVDF-50 is steadily declining. Two different regimes can be

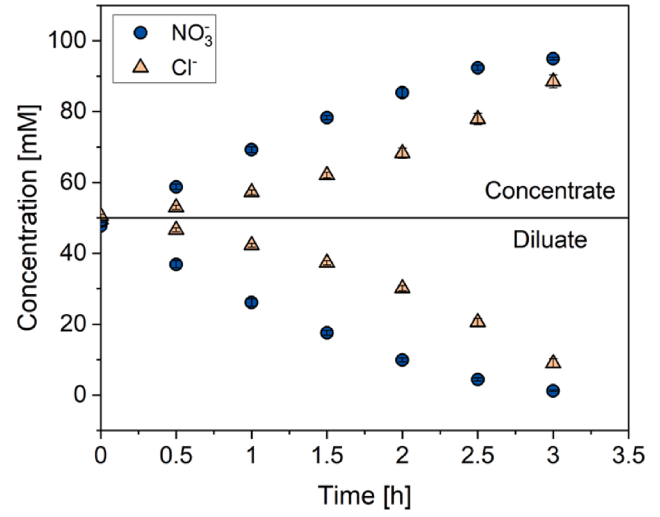

Fig. 5. Evolution of the nitrate and chloride concentration in the concentrate (top) and diluate (bottom) reservoir by ED with a CMX|PVDF-50|CMX|PVDF-50|CMX membrane stack. Experiments were conducted in triplicate.

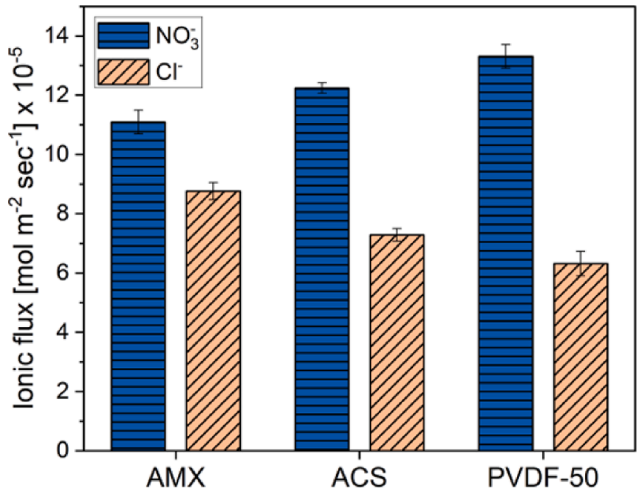

Fig. 6. Average ionic flux of nitrate and chloride obtained by ED using a membrane stack configuration of CMX|AEM|CMX|AEM|CMX, for the three selected AEMs: AMX, ACS, and PVDF-50. The measurements were conducted at a current density of 20 A·m^{-2}.

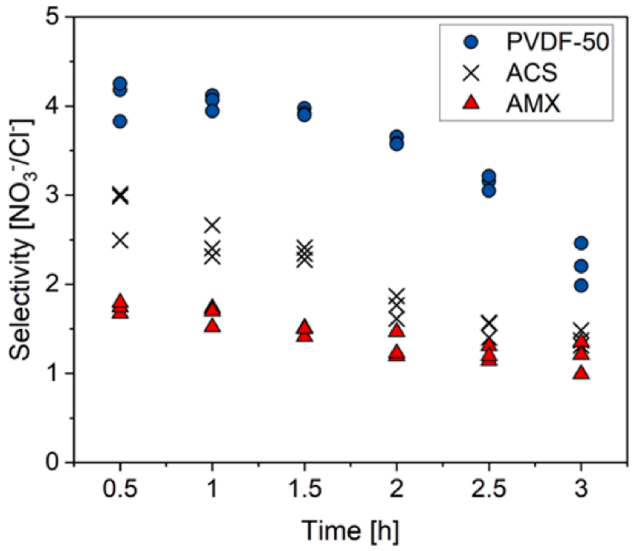

Fig. 7. Evolution of the nitrate over chloride selectivity by ED with a CMX|AEM|CMX|AEM|CMX membrane stack for three selected AEMs: AMX, ACS, and PVDF-50 at 20 A·m^{-2}. For each membrane, the experiments were repeated three times.

distinguished. The first one spans from 0 h to 2 h, during which the selectivity remains relatively constant within the range of 3.7–4. The second regime (t > 2 h) exhibits a more pronounced reduction. The observed decrease after two hours of the experiments can be attributed to the substantial removal of nitrate from the diluate stream and, consequently, the potential emergence of concentration polarization phenomena. PVDF-50, therefore, presents a superior behavior compared to the other two membranes, which is also evident by analyzing the trends of the recovery ratio of nitrate and chloride reported in Fig. 8, with PVDF-50 presenting a higher recovery for nitrate compared to those of ACS and AMX.

When comparing the energy consumption values, PVDF-50 exhibits a slightly higher value than ACS and AMX, as indicated in Table 3.

Nevertheless, this slight increase in energy consumption is a reasonable trade-off considering the membrane's superior nitrate selectivity. The enhanced selectivity for nitrate can be attributed to the

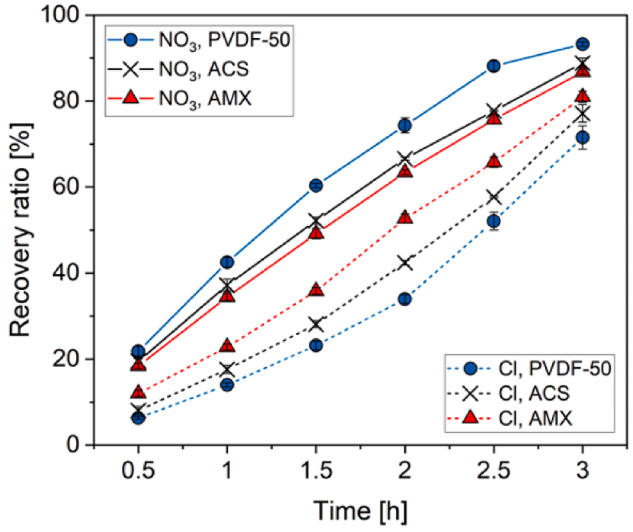

Fig. 8. Evolution of the recovery ratio of nitrate (solid lines) and chloride (dashed lines) by ED with a CMX|AEM|CMX|AEM|CMX membrane stack for three selected AEMs: AMX, ACS, and PVDF-50 at 20 A·m^{-2}. For each membrane, the experiments were repeated three times.

Table 3
Energy consumption obtained for the batch-mode ED experiments at 20 A·m^{-2} for the membranes PVDF-50, ACS, and AMX.

	PVDF-50	ACS	AMX
E (kJ·g^{-1} NO_3)	0.57	0.48	0.45
E (kWh·m^{-3})	0.92	0.75	0.68

increased hydrophobic nature of the membrane, as highlighted by the measurements of contact angles through captive bubble method, compared to the two commercial membranes. This characteristic promotes the permeation of less hydrated ions, such as nitrate, by requiring less energy to enter the membrane due to easier dehydration. Moreover, the increased hydrophobic environment within the membrane can also affect the mobility of ions with higher hydration energy, such as chloride, which are impeded by the hydrophobic structure [13].

Studies on the ACS membrane reported that the highly cross-linked surface layer on the membrane was responsible for the steric sieving of monovalent over divalent ions due to their different hydrated radii [27,29]. Despite the minimal difference in the hydrated radii of nitrate and chloride, [39] (Table 1) we do find that ACS presents a higher selectivity than AMX, an AEM that does not possess a cross-linked surface layer. Furthermore, Hawks *et al.* [53], proposed that the solvation structure of ions is another crucial parameter influencing the steric sieving mechanism. Indeed, while investigating the adsorption mechanisms of nitrate and chloride in ultramicroporous carbon during capacitive deionization, they ascribed the preference for nitrate adsorption to differences in the solvation structure and hydration energy of the two ions. Indeed, despite the similarity in their hydrated radii, nitrate's trigonal planar molecular geometry results in its preferential solvation around the edges, rather than on the planar faces, while chloride maintains symmetry across all three spatial dimensions. These structural characteristics, combined with the ~ 12 % lower hydration energy of nitrate – increasing the ability to alter its solvation structure when entering narrow pores – was reported to be the driving force behind the preferential adsorption of nitrate, and can be used to explain the higher nitrate selectivity of the ACS membrane compare to the AMX.

The most recent study examining nitrate and chloride transport in an electrodialysis (ED) setup was conducted by Mubita *et al.* [41]. In the present study, we maintained identical conditions regarding ion concentration in the solution, current density, and experiment duration, enabling a direct comparison of results. The membrane selectivity value reported by Mubita *et al.* for a heterogeneous anion-exchange membrane made with ion-exchange resins featuring quaternary ammonium groups with propyl substituents, ranged from 2.5 to 3. This range is lower than the selectivity values reported in our current study.

In order to assess whether the current density influences the performance of PVDF-50, batch-mode ED experiments were conducted at double the current density. In Fig. 9, the recovery ratio of nitrate and chloride for the two sets of experiments, 20 A·m^{-2} and 40 A·m^{-2}, are reported over the amount of charge passing through the membrane at the time of the sampling. Indeed, with the current doubled, the experiment's duration is halved, allowing correlation between the two trends using the transferred charge quantity. As can be observed from Fig. 9, the trends for nitrate and chloride for the two current densities are quite similar.

3.2.2. *Nitrate-selectrodialysis (NO_3-SED)*

In this section, we present the experimental results and performance of the nitrate-selectrodialysis (NO_3-SED) system, which is schematically represented in Fig. 2. As described in Section 2.5, the system exploits the difference in the nitrate over chloride selectivity of two different membranes, *i.e.* PVDF-50 and AMX. The membrane choices were made based on the insights obtained from the batch-mode electrodialysis (Section 3.2.1), with PVDF-50 exhibiting superior nitrate selectivity and AMX having the lowest.

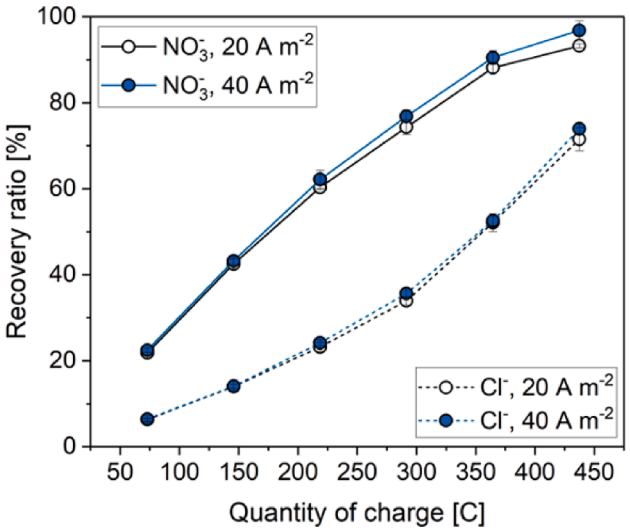

Fig. 9. Nitrate and chloride recovery ratio for the ED experiments at 20 and 40 A·m^{-2} as function of the amount of charge passing through the membrane. Experiments were conducted in triplicate.

The experiments were conducted three times and Fig. 10 illustrates the concentrations of nitrate and chloride in the two reservoirs, Feed 1 (Panel **A**) and Feed 2 (Panel **B**), over time. As anticipated, alternating between PVDF-50 and AMX membranes enables us to increase the nitrate concentration in Feed 2 while decreasing chloride concentration, whereas the opposite occurs in Feed 1. For experiments conducted at 20 A·m^{-2}, we observed an approximately 6–7 % increase/decrease in anion concentration in the two streams, as shown in Fig. 10.

Doubling the current density results in an increase of the nitrate concentration in Feed 2 of approximately 10 %, accompanied by a subsequent decrease in chloride levels. Although these changes may be evaluated as modest, it is important to realize that with advancements in membrane technology, there is potential for further improvements and achieving higher values in system performance. Additionally, to further explore the potential of this system, it may be worthwhile to explore alternative configurations, including the use of multiple reservoirs.

Finally, this strategy can be extended to other scenarios such as the selective separation of potassium from sodium [16,54], by alternating cation-exchange membranes, each with a different selectivity towards one of the two ions. When comparing the energy consumption of the experiments, it is possible to observe from Table 4 that the experiments conducted at 40 A·m^{-2} require more than four times the energy of those at a lower current density.

Exploiting the difference in the hydration energy of ions appears to be an interesting approach, and designing membranes that promote this effect have the potential to control and yield high ion selectivity. Various strategies can be pursued and eventually combined to further magnify the impact. For example, Mubita *et al.* [15] report on enhancing nitrate transport upon increasing the hydrophobicity of the membrane, by using resins containing different quaternary ammonium groups with alkyl chain length. Similarly, in our previous work [33], we report on a comparable effect by increasing the concentration of PVDF within the membrane. Additionally, the higher selectivity of the ACS membrane compared to the one of AMX observed in this study suggests that the presence of a crosslinked layer on the surface of the membranes promote the permeation of nitrate over chloride. We therefore believe that future membranes incorporating all these effects are key to achieving high separation values.

4. Conclusion

In terms of the selective separation of nitrate from chloride the performance of a recently introduced PVDF-based anion exchange membrane, PVDF-50, was tested for the first time in an electrodialysis setup, operating in batch mode. Our results demonstrate that this membrane exhibits higher and more stable nitrate over chloride selectivity values compared to two commercial membranes, surpassing the highest reported values in the literature. Additionally, we found that the current density does not significantly influence the performance of PVDF-50, enabling a reduction in operational time or installed membrane area.

However, it is important to note that this system cannot entirely prevent the transport of chloride to the concentrate stream. To mitigate this limitation, and selectively separate nitrate from chloride, we

Table 4
Energy consumption obtained for the batch-mode nitrate-selectrodialysis (NO_3-SED) experiments at 20 and 40 A·m^{-2}.

	20 A·m^{-2}	40·A/m^{-2}
Energy consumption (kJ·g^{-1} NO_3)	3.6	9.4

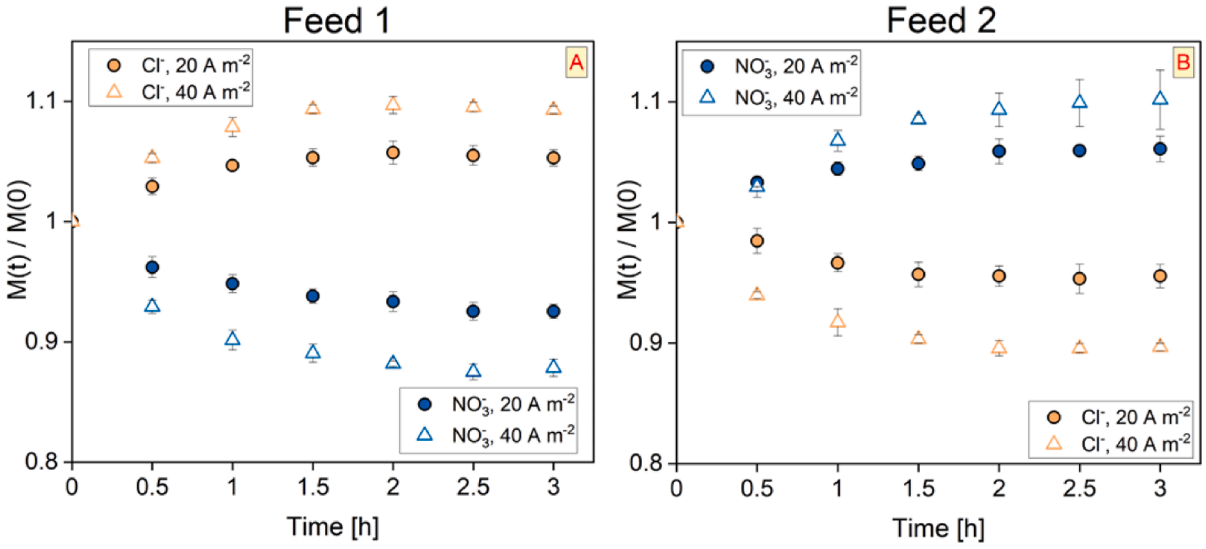

Fig. 10. Nitrate and chloride concentration variation in Feed 1 (A) and Feed 2 (B) for the selectrodialysis experiments conducted at the current density of 20 and 40 A·m^{-2}.

investigate the approach of alternating a series of AEMs with different nitrate selectivity (PVDF-50 and AMX), which we referred to as nitrate-selectrodialysis (NO_3-SED). Our findings indicate that with this system, it is possible to increase the concentration of nitrate while concurrently decreasing the concentration of chloride by approximately 10–11 % when operating at 40 $A{\cdot}m^{-2}$.

We believe that fine-tuning the chemical properties of membranes will become increasingly important for advancements in membrane technology, enabling further enhancement of selectivity. Such developments are not only relevant for the field of nitrate recovery but also for applications where the reduction of chloride concentration is of significant importance.

CRediT authorship contribution statement

Daniele Chinello: Writing – review & editing, Writing – original draft, Methodology, Investigation, Data curation. **Louis C.P.M. de Smet:** Writing – review & editing, Supervision. **Jan Post:** Writing – review & editing, Supervision.

Declaration of competing interest

The authors declare that they have no known competing financial interests or personal relationships that could have appeared to influence the work reported in this paper.

Acknowledgments

The authors thank the Dutch Research Council – Wetsus Partnership Programme on Sustainable Water Technology for funding this project (ALWET.2019.004). This work was performed in the cooperation framework of Wetsus, European Centre of Excellence for Sustainable Water Technology (www.wetsus.nl). Wetsus is co-funded by the Dutch Ministry of Economic Affairs and Ministry of Infrastructure and Environment, the European Union Regional Development Fund, the Province of Fryslan and the Northern Netherlands Provinces. The authors like to thank the participants of the research theme “Desalination & Concentrates” for the fruitful discussions and their financial support. We also would like to thank Eirini Aikaterini Gkougkousi and Tesse van der Wal for their precious contributions to the experimental work and Rodrigo Nobre for his invaluable support in the measurement of contact angles.

Appendix A. Supplementary data

Supplementary data to this article can be found online at https://doi.org/10.1016/j.seppur.2024.126885.

References

[1] “World Population Prospects - Population Division - United Nations.” Accessed: Aug. 10, 2023. [Online]. Available: https://population.un.org/wpp/.
[2] H. Cui, et al., Effects of nitrogen forms on nitrogen utilization, yield, and quality of two wheat varieties with different gluten characteristics, Eur. J. Agron. 149 (Sep. 2023) 126919, https://doi.org/10.1016/j.eja.2023.126919.
[3] P. Carillo, Y. Rouphael, Nitrate uptake and use efficiency: pros and cons of chloride interference in the vegetable crops, Front. Plant Sci. 13 (Jun. 2022) 899522, https://doi.org/10.3389/fpls.2022.899522.
[4] R. Kornijów, Eutrophication and derivative concepts. origins, compatibility and unresolved issues, *Ecohydrol. Hydrobiol.*, Jul. (2023), https://doi.org/10.1016/j.ecohyd.2023.07.001.
[5] E. Liu, et al., Effects of heavy metals on denitrification processes in water treatment: a review, Sep. Purif. Technol. 299 (Oct. 2022) 121793, https://doi.org/10.1016/j.seppur.2022.121793.
[6] L. Zhang, et al., Denitrification mechanism and artificial neural networks modeling for low-pollution water purification using a denitrification biological filter process, Sep. Purif. Technol. 257 (Feb. 2021) 117918, https://doi.org/10.1016/j.seppur.2020.117918.
[7] D. Chinello, A. Myrstad, L.C.P.M. de Smet, H. Miedema, Modelling the required membrane selectivity for $NO3^-$ recovery from effluent also containing Cl^-, while saving water, Chem. Eng. Res. Des. 193 (May 2023) 409–419, https://doi.org/10.1016/j.cherd.2023.03.038.
[8] C. van der Salm, W. Voogt, E. Beerling, J. van Ruijven, E. van Os, Minimising emissions to water bodies from NW european greenhouses; with focus on dutch vegetable cultivation, Agric Water Manag 242 (Dec. 2020) 106398, https://doi.org/10.1016/j.agwat.2020.106398.
[9] T. Luo, F. Roghmans, M. Wessling, Ion mobility and partition determine the counter-ion selectivity of ion exchange membranes, J. Membr. Sci. 597 (Mar. 2020) 117645, https://doi.org/10.1016/j.memsci.2019.117645.
[10] X. Pang, et al., Preparation of monovalent cation perm-selective membranes by controlling surface hydration energy barrier, Sep. Purif. Technol. 270 (Sep. 2021) 118768, https://doi.org/10.1016/j.seppur.2021.118768.
[11] W. Wang, et al., Recent advances in monovalent ion selective membranes towards environmental remediation and energy harvesting, Sep. Purif. Technol. 297 (Sep. 2022) 121520, https://doi.org/10.1016/j.seppur.2022.121520.
[12] N. Zhang, et al., Pressure-driven Li+/Mg2+ selective permeation through size-sieving nanochannels: the role of the second hydration shell, Sep. Purif. Technol. 327 (Dec. 2023) 124818, https://doi.org/10.1016/j.seppur.2023.124818.
[13] Ö. Tekinalp, P. Zimmermann, O.S. Burheim, L. Deng, Designing monovalent selective anion exchange membranes for the simultaneous separation of chloride and fluoride from sulfate in an equimolar ternary mixture, J. Membr. Sci. 666 (Jan. 2023) 121148, https://doi.org/10.1016/j.memsci.2022.121148.
[14] T. Kikhavani, S.N. Ashrafizadeh, B. Van Der Bruggen, Nitrate selectivity and transport properties of a novel anion exchange membrane in electrodialysis, Electrochim. Acta 144 (2014) 341–351, https://doi.org/10.1016/j.electacta.2014.08.012.
[15] T. Mubita, S. Porada, P. Aerts, A. van der Wal, Heterogeneous anion exchange membranes with nitrate selectivity and low electrical resistance, J. Membr. Sci. 607 (2020) 118000, https://doi.org/10.1016/j.memsci.2020.118000.
[16] Z. Qian, H. Miedema, S. Sahin, L.C.P.M. de Smet, E.J.R. Sudhölter, Separation of alkali metal cations by a supported liquid membrane (SLM) operating under electro dialysis (ED) conditions, Desalination 495 (Dec. 2020), https://doi.org/10.1016/j.desal.2020.114631.
[17] Z. Qian, H. Miedema, L.C.P.M. de Smet, E.J.R. Sudhölter, Permeation selectivity in the electro-dialysis of mono- and divalent cations using supported liquid membranes, Desalination 521 (Jan. 2022), https://doi.org/10.1016/j.desal.2021.115398.
[18] Y. Wang, W. Zhang, X. Zeng, T. Deng, J. Wang, Membranes for separation of alkali/alkaline earth metal ions: a review, Sep. Purif. Technol. 278 (Dec. 2021) 119640, https://doi.org/10.1016/j.seppur.2021.119640.
[19] R. Epsztein, E. Shaulsky, M. Qin, M. Elimelech, Activation behavior for ion permeation in ion-exchange membranes: role of ion dehydration in selective transport, J. Membr. Sci. 580 (January) (2019) 316–326, https://doi.org/10.1016/j.memsci.2019.02.009.
[20] Ö. Tekinalp, P. Zimmermann, S. Holdcroft, O.S. Burheim, L. Deng, Cation exchange membranes and process optimizations in electrodialysis for selective metal separation: a review, Membranes 13 (6) (May 2023) 566, https://doi.org/10.3390/membranes13060566.
[21] Y. Cheng, et al., Ionic transport and sieving properties of sub-nanoporous polymer membranes with tunable Channel size, ACS Appl. Mater. Interfaces 13 (7) (Feb. 2021) 9015–9026, https://doi.org/10.1021/acsami.0c22689.
[22] T. Sata, Studies on anion exchange membranes having permselectivity for specific anions in electrodialysis - effect of hydrophilicity of anion exchange membranes on permselectivity of anions, J. Membr. Sci. 167 (1) (2000) 1–31, https://doi.org/10.1016/S0376-7388(99)00277-X.
[23] M. Higa, et al., Electrodialytic properties of aromatic and aliphatic type hydrocarbon-based anion-exchange membranes with various anion-exchange groups, Polymer 55 (16) (Aug. 2014) 3951–3960, https://doi.org/10.1016/j.polymer.2014.06.072.
[24] C.X. Lin, et al., Side-chain-type anion exchange membranes bearing pendant quaternary ammonium groups via flexible spacers for fuel cells, J. Mater. Chem. A 4 (36) (Sep. 2016) 13938–13948, https://doi.org/10.1039/C6TA05090E.
[25] K. Chang, T. Xue, G.M. Geise, Increasing salt size selectivity in low water content polymers via polymer backbone dynamics, J. Membr. Sci. 552 (Apr. 2018) 43–50, https://doi.org/10.1016/j.memsci.2018.01.057.
[26] M. Irfan, L. Ge, Y. Wang, Z. Yang, T. Xu, Hydrophobic side chains impart anion exchange membranes with high monovalent-divalent anion selectivity in electrodialysis, ACS Sustainable Chem. Eng. 7 (4) (Feb. 2019) 4429–4442, https://doi.org/10.1021/acssuschemeng.8b06426.
[27] T. Luo, S. Abdu, M. Wessling, Selectivity of ion exchange membranes: a review, J. Membr. Sci. 555 (December 2017) (2018) 429–454, https://doi.org/10.1016/j.memsci.2018.03.051.
[28] D. Zhang, et al., Electro-driven in situ construction of functional layer using amphoteric molecule: the role of tryptophan in ion sieving, ACS Appl. Mater. Interfaces 11 (40) (Oct. 2019) 36626–36637, https://doi.org/10.1021/acsami.9b11163.
[29] S. Sarkar, P. Patnaik, R. Mondal, U. Chatterjee, Cross-linked, monovalent selective anion exchange membrane: effect of prealkylation and co-ions on selectivity, ACS Appl. Polym. Mater. 5 (3) (Mar. 2023) 1977–1988, https://doi.org/10.1021/acsapm.2c02045.
[30] Y. Zhao, et al., Robust multilayer graphene-organic frameworks for selective separation of monovalent anions, ACS Appl. Mater. Interfaces 10 (21) (May 2018) 18426–18433, https://doi.org/10.1021/acsami.8b03839.
[31] Y. Zhao, N. Mamrol, W.A. Tarpeh, X. Yang, C. Gao, B. Van der Bruggen, Advanced ion transfer materials in electro-driven membrane processes for sustainable ion-resource extraction and recovery, Prog. Mater Sci. 128 (Jul. 2022) 100958, https://doi.org/10.1016/j.pmatsci.2022.100958.

[32] X. Xiao, et al., Anion permselective membranes with chemically-bound carboxylic polymer layer for fast anion separation, J. Membr. Sci. 614 (Nov. 2020) 118553, https://doi.org/10.1016/j.memsci.2020.118553.
[33] D. Chinello, J. Post, L.C.P.M. de Smet, Selective separation of nitrate from chloride using PVDF-based anion-exchange membranes, Desalination 572 (Mar. 2024) 117084, https://doi.org/10.1016/j.desal.2023.117084.
[34] Y. Zhang, S. Paepen, L. Pinoy, B. Meesschaert, B. Van der Bruggen, Selectrodialysis: fractionation of divalent ions from monovalent ions in a novel electrodialysis stack, Sep. Purif. Technol. 88 (Mar. 2012) 191–201, https://doi.org/10.1016/j.seppur.2011.12.017.
[35] A.H. Galama, G. Daubaras, O.S. Burheim, H.H.M. Rijnaarts, J.W. Post, Fractioning electrodialysis: a current induced ion exchange process, Electrochim. Acta 136 (Aug. 2014) 257–265, https://doi.org/10.1016/j.electacta.2014.05.104.
[36] C. Jiang, et al., Ion-'distillation' for isolating lithium from lake brine, AIChE J 68 (6) (2022) e17710, https://doi.org/10.1002/aic.17710.
[37] W. Zhao, B. Yan, Z.J. Ren, S. Wang, Y. Zhang, H. Jiang, Highly selective butyric acid production by coupled acidogenesis and ion substitution electrodialysis, Water Res. 226 (Nov. 2022) 119228, https://doi.org/10.1016/j.watres.2022.119228.
[38] Y. Zhang, Y. Chen, M. Yue, W. Ji, Recovery of L-lysine from L-lysine monohydrochloride by ion substitution using ion-exchange membrane, Desalination 271 (1) (Apr. 2011) 163–168, https://doi.org/10.1016/j.desal.2010.12.016.
[39] E.R. Nightingale, Phenomenological theory of ion solvation. effective radii of hydrated ions, J. Phys. Chem. 63 (9) (Sep. 1959) 1381–1387, https://doi.org/10.1021/j150579a011.
[40] P. Dlugolecki, K. Nymeijer, S. Metz, M. Wessling, Current status of ion exchange membranes for power generation from salinity gradients, J. Membr. Sci. 319 (1–2) (Jul. 2008) 214–222, https://doi.org/10.1016/j.memsci.2008.03.037.
[41] T.M. Mubita, S. Porada, P.M. Biesheuvel, A. van der Wal, J.E. Dykstra, Strategies to increase ion selectivity in electrodialysis, Sep. Purif. Technol. 292 (Jul. 2022) 120944, https://doi.org/10.1016/j.seppur.2022.120944.
[42] Q.-B. Chen, Z.-Y. Ji, J. Liu, Y.-Y. Zhao, S.-Z. Wang, J.-S. Yuan, Development of recovering lithium from brines by selective-electrodialysis: effect of coexisting cations on the migration of lithium, J. Membr. Sci. 548 (Feb. 2018) 408–420, https://doi.org/10.1016/j.memsci.2017.11.040.
[43] D. Pintossi, C.-L. Chen, M. Saakes, K. Nijmeijer, Z. Borneman, Influence of sulfate on anion exchange membranes in reverse electrodialysis, npj clean, Water 3 (1) (Jun. 2020) 29, https://doi.org/10.1038/s41545-020-0073-7.
[44] P.A. Sosa-Fernández, J.W. Post, H.L. Nabaala, H. Bruning, H. Rijnaarts, Experimental evaluation of anion exchange membranes for the desalination of (waste) water produced after polymer-flooding, Membranes 10 (11) (Nov. 2020) 352, https://doi.org/10.3390/membranes10110352.
[45] R.S. Kingsbury, K. Bruning, S. Zhu, S. Flotron, C.T. Miller, O. Coronell, Influence of water uptake, charge, manning parameter, and contact angle on water and salt transport in commercial ion exchange membranes, Ind. Eng. Chem. Res. 58 (40) (Oct. 2019) 18663–18674, https://doi.org/10.1021/acs.iecr.9b04113.
[46] G. Sriram, et al., Recent progress in anion exchange membranes (AEMs) in water electrolysis: synthesis, physio-chemical analysis, properties, and applications, J. Mater. Chem. A 11 (39) (2023) 20886–21008, https://doi.org/10.1039/D3TA04298G.
[47] E. Güler, W. Van Baak, M. Saakes, K. Nijmeijer, Monovalent-ion-selective membranes for reverse electrodialysis, J. Membr. Sci. 455 (Apr. 2014) 254–270, https://doi.org/10.1016/j.memsci.2013.12.054.
[48] S.A. Mareev, D.Y. Butylskii, N.D. Pismenskaya, C. Larchet, L. Dammak, V. V. Nikonenko, Geometric heterogeneity of homogeneous ion-exchange neosepta membranes, J. Membr. Sci. 563 (Oct. 2018) 768–776, https://doi.org/10.1016/j.memsci.2018.06.018.
[49] P. Długołęcki, P. Ogonowski, S.J. Metz, M. Saakes, K. Nijmeijer, M. Wessling, On the resistances of membrane, diffusion boundary layer and double layer in ion exchange membrane transport, J. Membr. Sci. 349 (1–2) (Mar. 2010) 369–379, https://doi.org/10.1016/j.memsci.2009.11.069.
[50] W. Wang, et al., Evaluation of the ideal selectivity and the performance of selectrodialysis by using TFC ion exchange membranes, J. Membr. Sci. 582 (Jul. 2019) 236–245, https://doi.org/10.1016/j.memsci.2019.04.007.
[51] H. Luo, W.-A.-S. Agata, G.M. Geise, Connecting the ion separation factor to the sorption and diffusion selectivity of ion exchange membranes, Ind. Eng. Chem. Res. 59 (32) (Aug. 2020) 14189–14206, https://doi.org/10.1021/acs.iecr.0c02457.
[52] P.M. Biesheuvel, S. Porada, M. Elimelech, J.E. Dykstra, Tutorial review of reverse osmosis and electrodialysis, J. Membr. Sci. 647 (Apr. 2022) 120221, https://doi.org/10.1016/j.memsci.2021.120221.
[53] S.A. Hawks, et al., Using ultramicroporous carbon for the selective removal of nitrate with capacitive deionization, Environ. Sci. Tech. (2019), https://doi.org/10.1021/acs.est.9b01374.
[54] Z. Qian, H. Miedema, L.C.P.M. de Smet, E.J.R. Sudhölter, Modelling the selective removal of sodium ions from greenhouse irrigation water using membrane technology, Chem. Eng. Res. Des. 134 (Jun. 2018) 154–161, https://doi.org/10.1016/j.cherd.2018.03.040.